occurs with greatest yield on the high-temperature sulfur phase. The fact that both reactions exhibit the same sensitivity to these surface characteristics suggests that the heterocyclization of acetylene is initiated by dimerization to form a C_4H_4 intermediate which then cyclizes with sulfur. Thiophene then desorbs from the surface in the temperature range 280–420 K. This surface chemistry offers a low-temperature route to the reduction of high surface sulfur coverages on the Pd(111) surface. The nature of the barrier to complete removal of surface sulfur is unknown; however, it is possible that at high pressures one might use this route to achieve complete regeneration of sulfur poisoned catalysts.

Acknowledgment. This work was supported by the Department of Energy under Grant No. DE-AC02-76ER01198 through the Materials Research Lab of the University of Illinois. A.J.G. holds a David and Lucile Packard Foundation Fellowship in Science and Engineering.

Registry No. C_4H_4S, 110-02-1; C_2H_2, 74-86-2.

Face-Specific Interactions of Anionic Sulfur Donors with Oriented Crystals of (0001) CdX (X = Se, S) and Correlation with Electrochemical Properties

James J. Hickman and Mark S. Wrighton*

Contribution from the Department of Chemistry, Massachusetts Institute of Technology, Cambridge, Massachusetts 02139. *Received September 17, 1990*

Abstract: Oriented (0001) CdX (X = S, Se) crystals selectively adsorb MoS_4^{2-} or $Et_2NCS_2^-$ onto the Cd-rich faces. Binding of the anions is effected by dipping the etched CdX crystals into CH_3CN containing 20 mM $[Et_4N]_2MoS_4$ or $Na[Et_2NCS_2]$. Removal of the crystal from the solution followed by rinsing with CH_3CN leaves MoS_4^{2-} or $Et_2NCS_2^-$ on the Cd-rich, but not X-rich, face of the crystal as detected by X-ray photoelectron spectroscopy (XPS) and Auger electron spectroscopy (AES). The specificity for Cd-face vs X-face binding is typically >5:1 as determined by XPS and AES data for both faces of the same crystal. S element maps for the MoS_4^{2-}-modified, Cd face of CdSe crystals reveal non-uniform binding of MoS_4^{2-}. There is a correlation of the regions of MoS_4^{2-} binding with the crystal planes revealed in the pretreatment/etch procedure. Studies of interfacial capacitance of CdX/electrolyte systems show strong interaction of MoS_4^{2-} selectively with the Cd-rich face, based on the relative flat-band shifts for the Cd- and X-rich faces when exposed to 10^{-2} M MoS_4^{2-}. However, repeated etching of the X-rich face with concentrated HCl reduces the degree of selectivity. The face-selective interaction of CdX with $Et_2NCS_2^-$ is also found from measures of the XPS and the photocurrent–voltage curves for the Cd- and S-rich faces. The binding sites for the anionic S donors are proposed to be exposed Cd^{2+} centers, but the etching of the (0001) surfaces prior to reaction exposes planes other than the Cd- or S-rich (0001) planes.

We wish to report that anionic S-containing species (MoS_4^{2-} and $Et_2NCS_2^-$) adsorb selectively on the etched Cd-rich faces of (0001) oriented single crystals of CdX (X = S, Se) and that the electrochemical properties of these crystals in solutions containing the adsorbate are directly related to the adsorption. We have used X-ray photoelectron spectroscopy (XPS), Auger electron spectroscopy (AES), differential capacitance, and photoelectrochemistry to demonstrate the face selectivity of adsorption of anionic S-containing species on CdX. Our work extends previous studies on the interaction of anionic S-donors such as dithiocarbamates,[1] thiolates,[2-4] and polysulfides[5-7] on the Cd-rich face of (0001) CdX crystals. Such studies reveal that anionic S donors can strongly and favorably influence the CdX/electrolyte interface energetics to give highly efficient photoelectrochemical devices.[1-3,5-7] It has also been reported that amines interact with the Cd-rich face, and such interactions can be exploited in sensor devices.[8]

Our new study was undertaken to better understand the role of crystal orientation in determining the degree of interaction of CdX with anionic S donors. One would expect different chemistry at the two faces of (0001) CdX, based on differences in structure and composition. Significant differences have been reported earlier.[9] In particular, differential capacitance measurements have shown that the Cd, but not S, face of (0001) CdS interacts strongly with S^{2-}.[10] More recently it has been shown that $Fe(CN)_6^{3-/4-}$ interacts more favorably with the Cd-rich face of CdX.[11] Also, it has been suggested that an ion-specific electrode could be based on the selective interaction of SH^- with the Cd face and Cd^{2+} with the S face of CdS.[12]

It is important to correlate interaction of anionic S-donor species with the electrochemical behavior of the crystals. A strong in-

* Address correspondence to this author.

(1) Thackeray, J. W.; Natan, M. J.; Ng, P.; Wrighton, M. S. *J. Am. Chem. Soc.* **1986**, *108*, 3570.
(2) Natan, M. J.; Thackeray, J. W.; Wrighton, M. S. *J. Phys. Chem.* **1986**, *90*, 4089.
(3) (a) Josseaux, P.; Kirsch-De Mesmaeker, A.; Riga, J.; Verbist, J. *J. Electrochem. Soc.* **1983**, *130*, 1067. (b) Aruchamy, A.; Venkatarathnam, A.; Subrahamnyam, M.; Subba Rao, G. V.; Aravamudan, G. *Electrochim. Acta* **1982**, 701.
(4) (a) Josseaux, P.; Kirsch-De Mesmaeker, A.; Roche, A.; Romand, M.; Montes, H. *J. Electrochem. Soc.* **1985**, *132*, 684. (b) Dewitt, R.; Kirsch-De Mesmaeker, A. *Appl. Phys. Lett.* **1984**, *45*, 145. (c) Dewitt, R.; Kirsch-De Mesmaeker, A. *J. Electrochem. Soc.* **1983**, *130*, 1995. (d) Kirsch-De Mesmaeker, A.; Josseaux, P.; Nasielski, J.; Defosse, C. *Solar Energy Mat.* **1982**, *6*, 429. (e) Kirsch-De Mesmaeker, A.; Decoster, A. M.; Nasielski, J. *Solar Energy Mat.* **1981**, *4*, 203.
(5) Ellis, A. B.; Kaiser, S. W.; Bolts, J. M.; Wrighton, M. S. *J. Am. Chem. Soc.* **1977**, *99*, 2839.
(6) Heller, A.; Chang, K. C.; Miller, B. *J. Electrochem. Soc.* **1977**, *124*, 697.
(7) Minoura, H.; Oki, T.; Tsuiki, M. *Chem. Lett.* **1976**, 1279.
(8) (a) Meyer, G. J.; Lisensky, G. C.; Ellis, A. B. *J. Am. Chem. Soc.* **1988**, *110*, 4914. (b) Lisensky, G. C.; Penn, R. L.; Murphy, C. J.; Ellis, A. B. *Science* **1990**, *248*, 840.
(9) (a) Woods, J. *Brit. J. Appl. Phys.* **1960**, *11*, 296. (b) Munir, Z. A.; Hirth, J. P. *J. Appl. Phys.* **1970**, *41*, 2697. (c) Munir, Z. A.; Seacrist, L. S.; Hirth, J. P. *Surf. Sci.* **1971**, *28*, 357.
(10) Minoura, H.; Wantanabe, T.; Oki, T.; Tsuiki, M. *Jpn. J. Appl. Phys.* **1977**, *16*, 865.
(11) Rubin, H. D.; Arent, D. J.; Humphrey, B. D.; Bocarsly, A. B. *J. Electrochem. Soc.* **1987**, *134*, 93.
(12) Uosaki, K.; Shigematsu, Y.; Kita, H.; Umezawa, Y. *Anal. Chem.* **1989**, *61*, 1980.

0002-7863/91/1513-4440$02.50/0

Scheme I. n-CdX at the Flat-Band Potential, $E_f = E_{FB}$, in an Innocent Electrolyte Solution (Left) and a Solution Containing an Anionic S Donor (Right)[a]

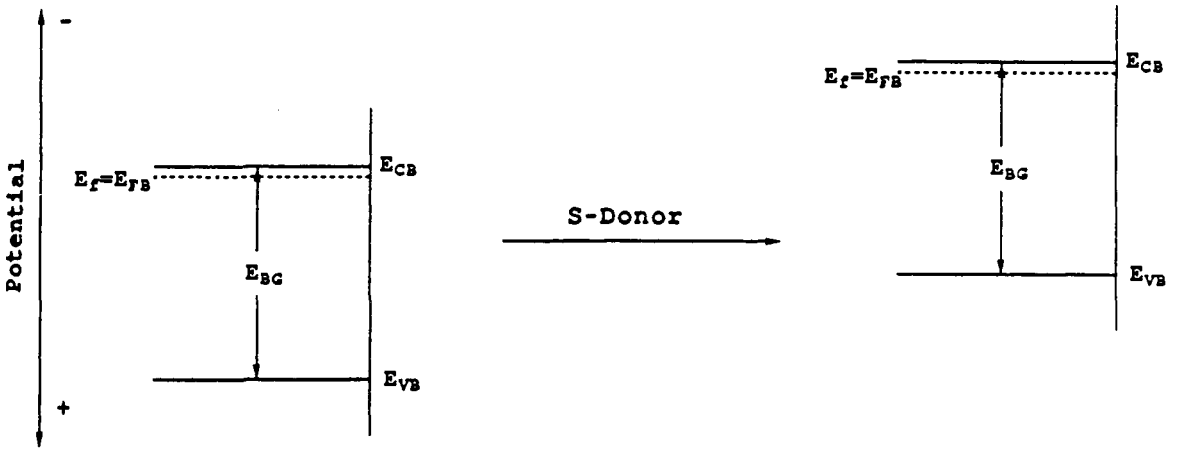

teraction can be reflected in significant changes in the flat-band potential, E_{FB}, of the semiconductor in electrolyte solutions containing the adsorbate. The negatively charged S donors yield negative shifts in E_{FB}[1,13] (Scheme I). We include herein a demonstration that results from shifts in E_{FB} can be correlated with data from surface analysis showing selective binding. We chose to investigate MoS_4^{2-} as an adsorbate because of its high charge-to-size ratio. We have also investigated $Et_2NCS_2^-$, because although previous work shows strong interaction at the Cd face of CdX, the interaction with the S-rich face was not investigated, and we wish to relate face-selective chemistry to the high efficiencies found for photoelectrochemical oxidation of $Et_2NCS_2^-$.[1]

Experimental Section

Chemicals. $Na[Et_2NCS_2]\cdot 3H_2O$ was obtained from Aldrich, $Na_2[MoS_4]$ was obtained from Alfa, and $NaClO_4$ (anhydrous) was obtained from G. Frederick Smith Chemicals. These chemicals were used as received. $[Et_4N]_2MoS_4$ was prepared by a method described by Hoffman.[14] Elemental analysis (Galbraith Labs) was satisfactory. Anal. Calc (found) for $C_{16}H_{40}N_2MoS_4$: C, 39.65 (39.68); H, 8.32 (8.34); N, 5.78 (5.76); S, 26.46 (26.45).

Single crystals of low-resistivity (1 Ω cm) n-CdS and n-CdSe, cut perpendicular to the *c* axis to expose the (0001) faces, were obtained from Cleveland Crystals (Cleveland, OH). The crystals were 1–2 mm thick and the (0001) faces were 1–2 cm^2 as received, and then were cut into 0.2–0.4 cm^2 pieces with a diamond-bladed string saw. The CdX crystals were cleaned in concentrated H_2SO_4 to remove carbon-containing deposits accumulated during the cutting process. The donor densities, N_D, determined from the slopes of Mott-Schottky plots, were typically 0.5–2 × 10^{16} for CdS and 1–10 × 10^{17} cm^{-3} for CdSe.

Surface Pretreatment, Modification, and Analysis. The CdS crystals were etched in 12 M HCl[15] for 30 s and rinsed with copious amounts of H_2O and then CH_3CN. The CdSe crystals were etched in a 3:1 mixture of $HCl:HNO_3$ for 15 s, rinsed with H_2O, and then exposed to a 1 M KCN solution for 5–10 min.[15] The crystals were finally rinsed with H_2O and then CH_3CN. AES analysis of the etched CdX crystals indicated the presence of some adventitious C and O, but no other contaminating elements were detected.

The CdX crystals were modified with MoS_4^{2-} by immersing them for 5 min in a 20 mM solution of $[Et_4N]_2MoS_4$ dissolved in distilled and deoxygenated CH_3CN. The crystals were then rinsed with CH_3CN for 1–2 min and stored under Ar prior to introduction into the XPS or Auger spectrometer. Similar procedures were used to investigate the selective binding of $Et_2CS_2^-$.

XPS data were taken on a SSL 100 spectrometer. Samples were attached to the stage via metal clips. The Cd $3d_{5/2}$ peak (405.1 eV binding energy) was monitored as the reference and was used to correct for sample charging. The X-ray line used for excitation was the Al Kα line at 1486.6 eV. Auger electron spectra were recorded on a PHI 660 Scanning Auger Microprobe employing a 15 keV, 10–20 nA electron beam for excitation. SEM micrographs were recorded on the same instrument at 15 keV and 1–2 nA electron beam excitation energy. Samples were attached and grounded to the stage with metal screws. AES and XPS reference data for Cd, S, Se, and Mo have been previously reported.[16]

Electrochemical Methods. The single-crystal electrodes were prepared by mounting such that either the shiny face of the etched crystal (the Cd-rich face), the dull face (the X-rich face), or both faces were exposed. Ohmic contact to the back or edge of the crystal to a flattened piece of Cu wire coated with Ag epoxy was made by a Ga–In eutectic mixture rubbed into the CdX surface. The Cu wire was encased in 3 mm glass tubing, ~10 cm long, and the electrode was sealed with clear epoxy so that only the desired crystal face(s) were exposed. Prior to any measurement or experiment, the electrodes were etched as described above. The reference electrode was a Ag/0.01 M $AgNO_3$/0.1 M $[n\text{-}Bu)_4N]ClO_4/CH_3CN$ electrode, and the counter electrode was a Pt gauze electrode of ~3 cm^2 area.

Differential capacitance measurements of CdX were obtained under Ar in the dark in a quiet solution, employing a PAR Model 5204 lock-in amplifier with an internal oscillator. A 5-mV peak-to-peak sine wave at 1–10 KHz was used as the AC modulation. The DC bias was provided by a PAR Model 173 potentiostat along with a PAR Model 175 programmer or with a Pine Instruments RDE-4 bipotentiostat, and data were recorded on a Kipp and Zonen BD91 *x–y* recorder. Capacitance values were extracted from the quadrature values by modeling as a simple resistance–capacitance circuit. A dummy resistance–capacitance circuit was used to calibrate the measurements. The data were analyzed with use of a Hewlett-Packard 85 computer and plotted with a Hewlett-Packard 1150 plotter.

Current–voltage measurements were obtained on a Pine Instruments RDE-4 bipotentiostat and recorded on a Kipp and Zonen BD91 *x–y* recorder. The light source for illumination of the n-CdS was an Ar laser operated at 486 nm. Light intensities were measured with a Tektronix J16 radiometer with a calibrated Solarex Corporation photometer. The intensities were varied with a photographic polarizing filter and precision diameter masks.

Results and Discussion

Scanning Electron Microscopy. Etching of CdX crystals originally oriented with the (0001) faces exposed yields textured surfaces revealing other planes. Figure 1 shows the (0001) surfaces of CdS after a typical etch procedure. Clearly, the surfaces available for adsorption that result from etching are not the (0001) surfaces. In fact, the etching itself is an excellent example of the differences in reactivity of different crystal faces.[9,15] Our findings (vide infra) support the conclusion that etching preferentially reveals sites, presumably coordinatively unsaturated Cd^{2+} centers,

(13) Gerischer, H. In *Physical Chemistry: An Advanced Treatise*; Eyring, H., Henderson, B., Jost, W., Eds.; Academic: New York, 1970; Vol. 9A.
(14) Friesen, G. D.; McDonald, J. W.; Newton, W. E.; Euler, W. B.; Hoffman, B. M. *Inorg. Chem.* **1983**, *22*, 2202.
(15) Gatos, H. C.; Lavine, M. C. In *Progress in Semiconductors*; Gibson, A. F., Burgess, R. E., Eds.; CRC Press: Cleveland, OH, 1965; Vol. 8, pp 36–42.
(16) AES and XPS reference data for Cd, S, Se, and Mo can be found in: *Handbook of Auger Electron Spectroscopy*; Perkin-Elmer, Corp.: Eden Prairie, MN, 1978 (AES). *Handbook of X-ray Photoelectron Spectroscopy*; Perkin-Elmer, Corp.: Eden Prairie, MN, 1979 (XPS).
(17) Nefedou, V. I.; Salyn, Ya. V.; Leonhardt, G.; Scheibe, R. *J. Electron Spectros.* **1977**, *10*, 121.

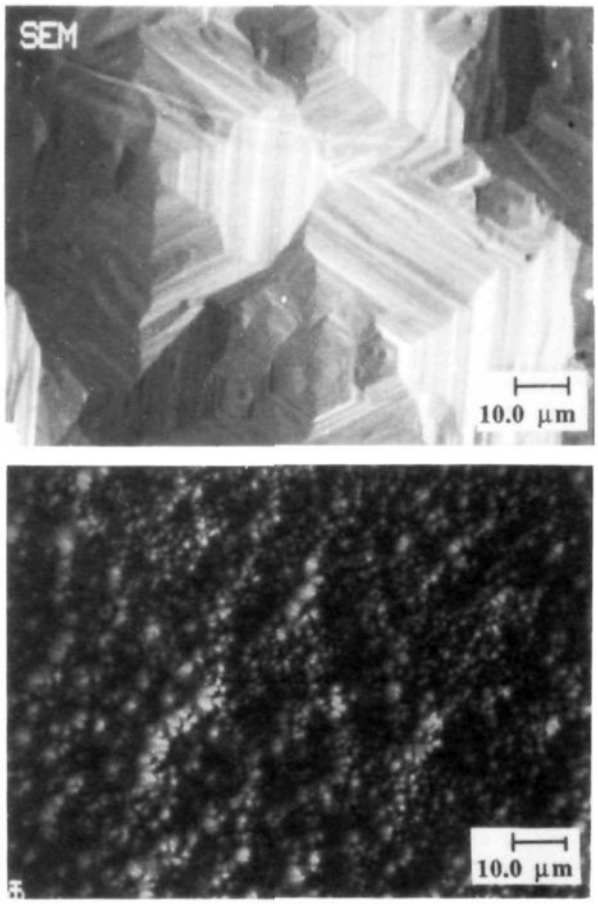

Figure 1. SEM micrographs of the Cd-rich face (top) and the S-rich face (bottom) of a CdS single crystal after etching for 30 s in 12 M HCl.

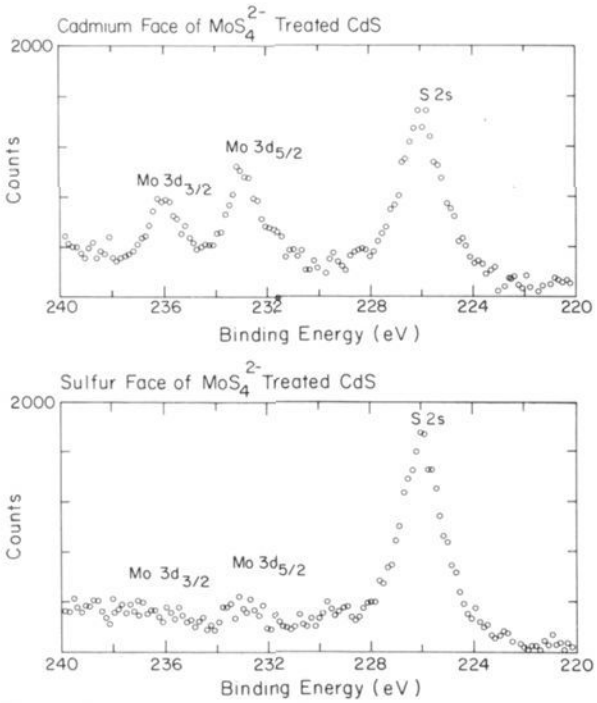

Figure 2. Comparison of XPS data for the Cd and S faces of (0001) CdS after treatment with MoS_4^{2-} showing MoS_4^{2-} adsorption on only the Cd-rich face.

upon etching the original Cd-rich (0001) CdX crystals. Persistent etching of the X-rich face also reveals binding sites, and this fact accounts for apparent irreproducibility in establishing face-selective

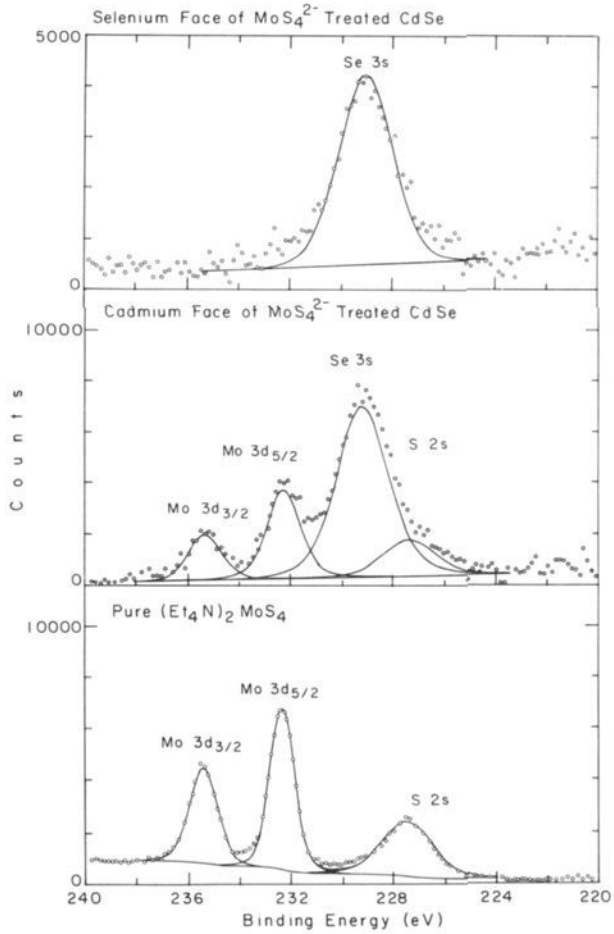

Figure 3. XPS data of the Se-rich face of CdSe which shows no MoS_4^{2-} adsorption (top), the Cd-rich face which shows Mo and S present in the proper proportions and energies for MoS_4^{2-} (middle), and an authentic sample of MoS_4^{2-} (bottom).

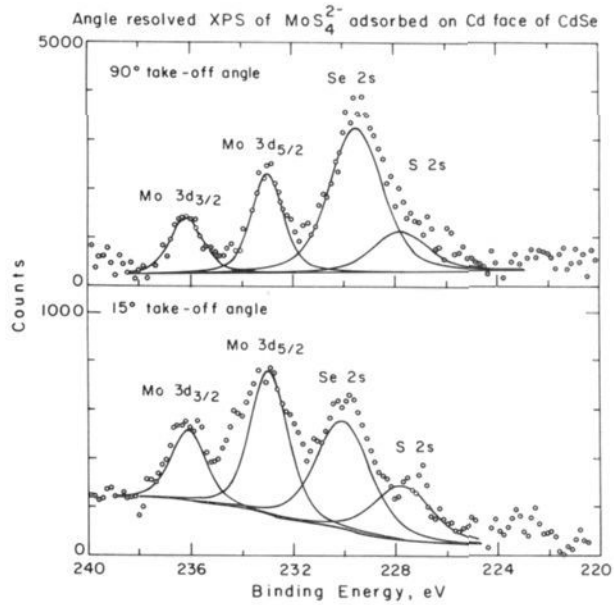

Figure 4. Angle-resolved XPS data for the MoS_4^{2-}-treated Cd face of (0001) CdSe at a 90° angle to the analyzer (top) and a 15° angle (bottom).

adsorption on oriented crystals of (0001) CdX.

Surface Analysis by XPS and AES. CdX crystals were examined by XPS and/or AES to determine if anionic S donors bind selectively to the Cd-rich face of (0001) CdX crystals. Etched

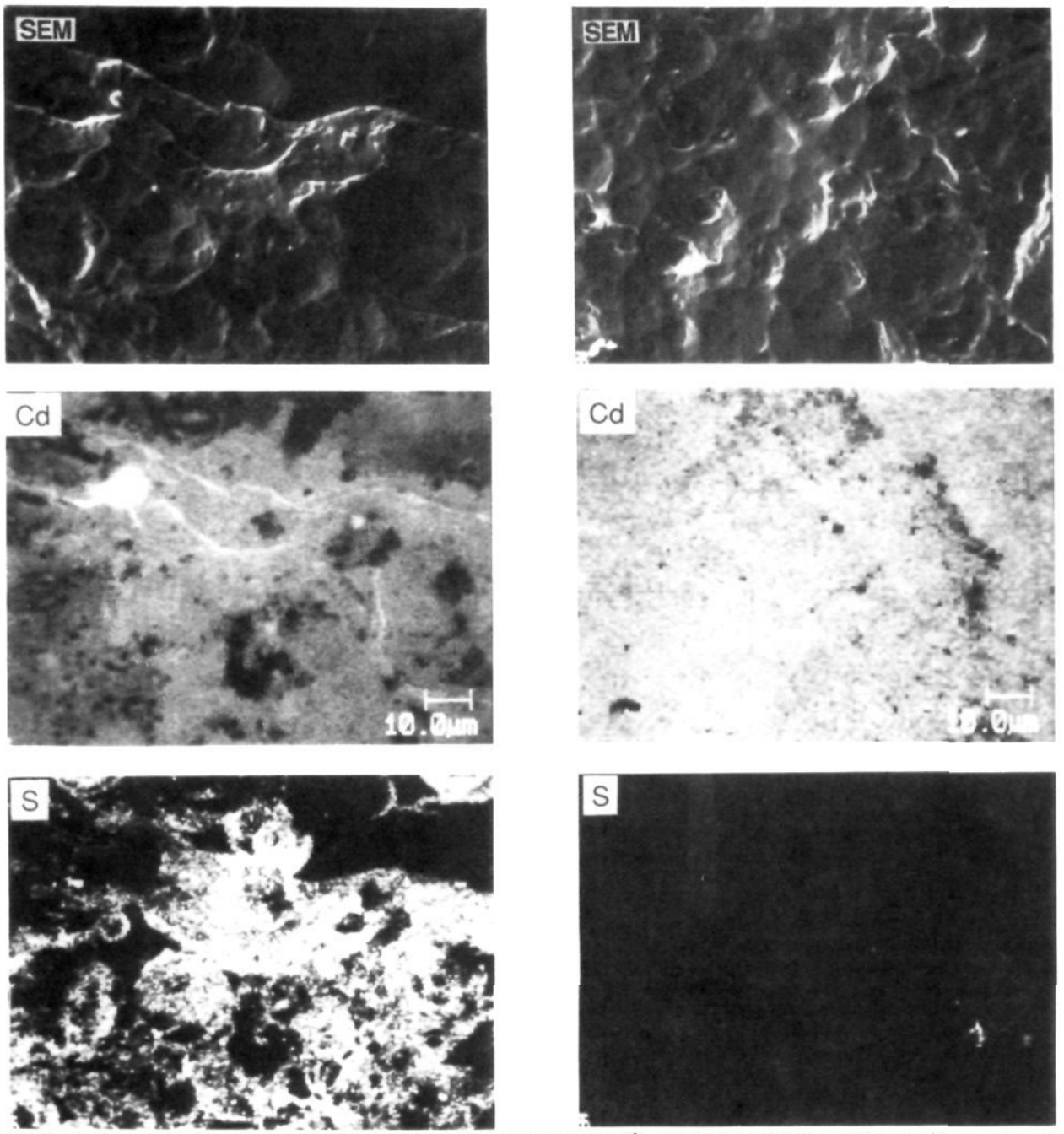

Figure 5. SEM and Auger element maps of a (0001) CdSe crystal modified with MoS_4^{2-}. The Cd (middle left) and S (lower left) element maps of the Cd-rich face of a (0001) CdSe single crystal shown in the SEM in the top left. On the right are the Cd and S element maps for the Se-rich face depicted in the SEM at the top right. Brighter regions in the element maps correspond to higher concentrations of the element. The Cd maps are uniform except for slight C contamination, indicating no differential charging. S (from adsorbed MoS_4^{2-}) is only detected on the Cd face and is non-uniform.

CdX crystals modified with MoS_4^{2-} were examined principally by XPS because the element Mo is much more easily detected by XPS than AES. CdSe crystals were examined by AES (for S) and XPS (for Mo and S). Both surface techniques demonstrate selective binding of MoS_4^{2-} to the Cd-rich face of CdX. Selective binding of $Et_2NCS_2^-$ was investigated for CdS with XPS, based on the unique element nitrogen.

Representative XPS data for CdS modified with MoS_4^{2-} are shown in Figure 2. Spectra were recorded for both the Cd and S faces of the same crystal to eliminate artifacts arising from differences between crystals. The same results were obtained for each of eight independently prepared samples. The Mo signal from the Cd-rich face is at least five times that arising from the S-rich face, and, in fact, for the CdS the Mo signal is not detectable above the noise from the S-rich face. The peak energy of the Mo $3d_{5/2}$ signal is 232.6 eV (using Cd^{2+} $4d_{5/2}$ at 405.1 eV as a reference) which is consistent with Mo(VI)[15] and suggests that MoS_4^{2-} remains intact after adsorption onto the surface of the crystal. Since the S 2s signal from the CdS dominates the S signal from MoS_4^{2-}, relative Mo to S ratios cannot be evaluated.

XPS establishes that MoS_4^{2-} also binds selectively on the Cd-rich face of (0001) CdSe (Figure 3). Though the key S peak overlaps the Se peak, the Mo/S ratio and peak positions in the XPS of MoS_4^{2-}-treated CdSe are consistent with intact MoS_4^{2-}, and demonstrate essentially the same pattern as indicated by the XPS spectrum of pure $[Et_4N]_2MoS_4$ (Figure 3). Angle-resolved XPS data for CdSe modified with MoS_4^{2-} show that the Mo is at the surface, but intense, good signal-to-noise data for the S could

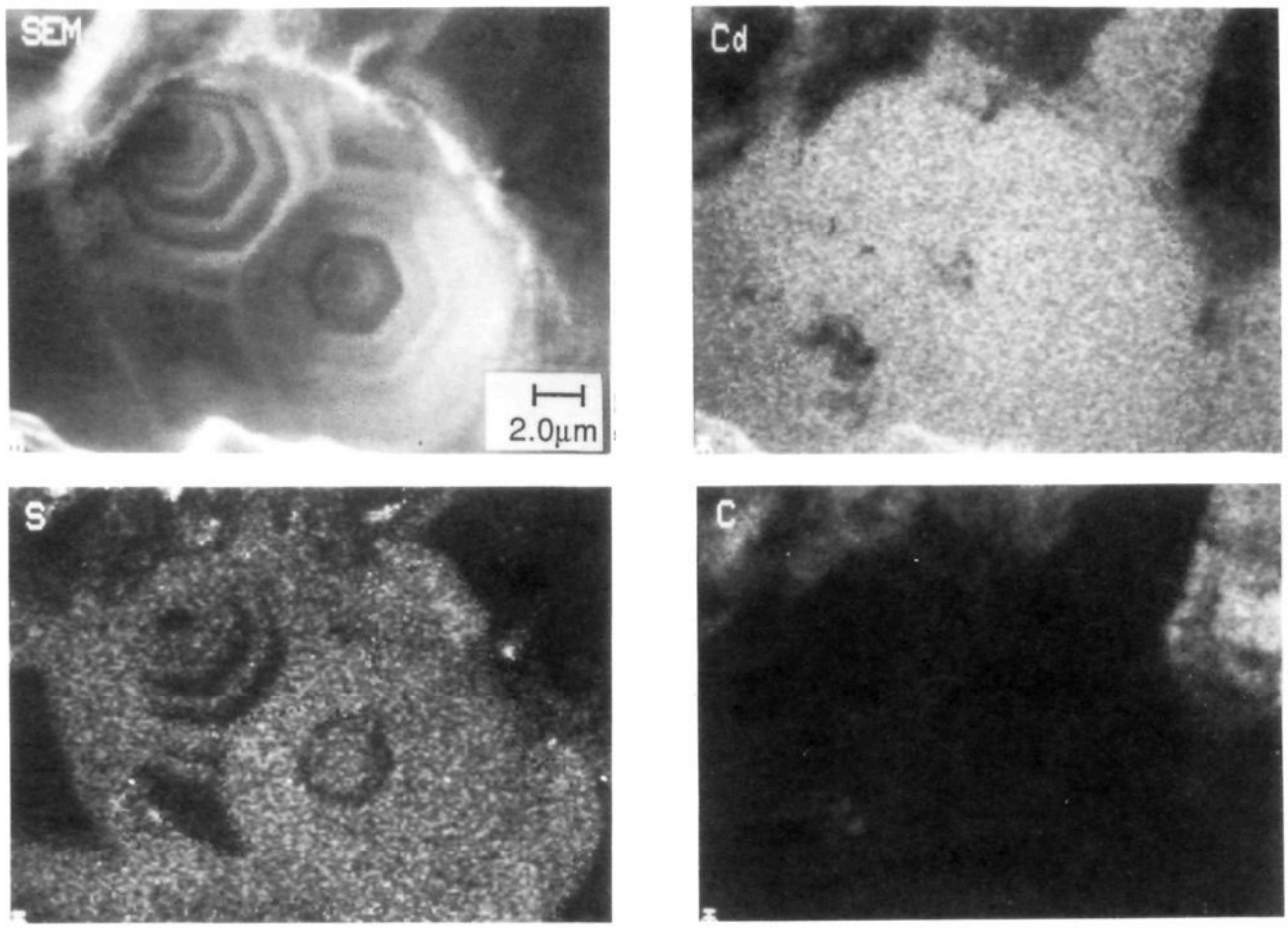

Figure 6. SEM and high lateral resolution Auger element maps (S, C, and Cd) of an etch-pit on the Cd-rich face of a MoS_4^{2-}-modified (0001) CdSe crystal. The S is due to adsorbed MoS_4^{2-}. The region shown is a higher magnification of a region of the crystal characterized in Figure 5. The surface concentration of the elements is proportional to the brightness in each photograph. Carbon is adventitious from exposure to atmosphere after MoS_4^{2-} interaction. Note the Cd signal is obscured where the C coverage appears large.

not be obtained, even for a grazing angle of 15° (Figure 4). In any event, the Cd-rich face of CdSe binds the MoS_4^{2-} selectively as established for six independently measured samples. The data in Figures 3 and 4 are representative and the selectivity is similar to that for CdS.

The S 2s peak (on CdS) and Se 3s peak (on CdSe) in XPS measurements were used to calibrate the absolute magnitude of the Mo 3d peaks, and we conclude that there is roughly one monolayer of MoS_4^{2-} on the Cd-rich face of (0001) CdX. Prolonged washing of MoS_4^{2-}-treated CdX with CH_3CN does lead to removal of the Mo signal. The results are consistent with reversible binding of intact MoS_4^{2-} to Cd^{2+} centers revealed by etching the Cd-rich face of (0001) CdX represented in eq 1.

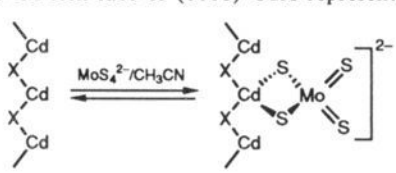

(1)

We have also examined CdSe single crystals by SEM and AES. Figure 5 shows SEM micrographs of the Cd- and Se-rich faces of (0001) CdSe modified with MoS_4^{2-}. As with XPS, by AES we find S on the Cd-rich face but not on the Se-rich face. However, one can see a pattern in the S map. The non-uniform map does not arise from C contamination or differential charging of the surface. The SEM of the Cd-rich face of CdSe in Figure 5 shows a surface with many sharp ridges, irregularities, and etch pits. If this surface is examined at a higher magnification (Figure 6), the etch pits are revealed to consist of planes of differing crystallographic orientation. Comparison of the S map from AES to the SEM indicates that the MoS_4^{2-} interacts only with certain features on the Cd-rich face of CdSe. Since the Cd map from AES is uniform over the region where there is significant variation of the S, the pattern of S AES signals cannot arise from differential charging. A second independently prepared sample is characterized by high lateral resolution AES (Figures 7 and 8). Figure 7 shows the S, Cd, and C maps, again showing non-uniform modification with MoS_4^{2-} correlated with the surface texture seen by SEM. To verify that the non-uniform binding is not due to massive over-adsorption on some planes and smaller, but at least monolayer adsorption on others, we looked at the relative compositions at various points on the Cd-rich face of the CdSe crystal characterized by data in Figure 7. Figure 8 shows survey scans of four points on the modified crystal. In areas where the presence of S is indicated (Figure 7), we find about a monolayer of S, and in areas which appear dark in the S map, we see little, if any, indication of MoS_4^{2-} binding. Thus, surface analysis results for etched (0001) CdSe show that MoS_4^{2-} adsorbs selectively on the etched Cd-rich face, but the binding on the etched Cd face is non-uniform.

Modification of etched (0001) CdS crystals with $Et_2NCS_2^-$ shows evidence of selective binding on the Cd face as deduced from XPS measurements of the N 1s signal. Figure 9 shows a representative comparison of the XPS data for the Cd face and the S face of the same crystal after modification with $Et_2NCS_2^-$. XPS data in the N 1s region are somewhat problematical, owing to the proximity of the Cd $4d_{5/2}$ peak. However, as shown in Figure 9, the data are compelling. The XPS of CdS exposed only to CH_3CN does not show a N 1s signal. Thus, the relative N 1s signals on the Cd and S faces of the CdS provide a good measure of the relative surface concentrations of $Et_2NCS_2^-$. The selective

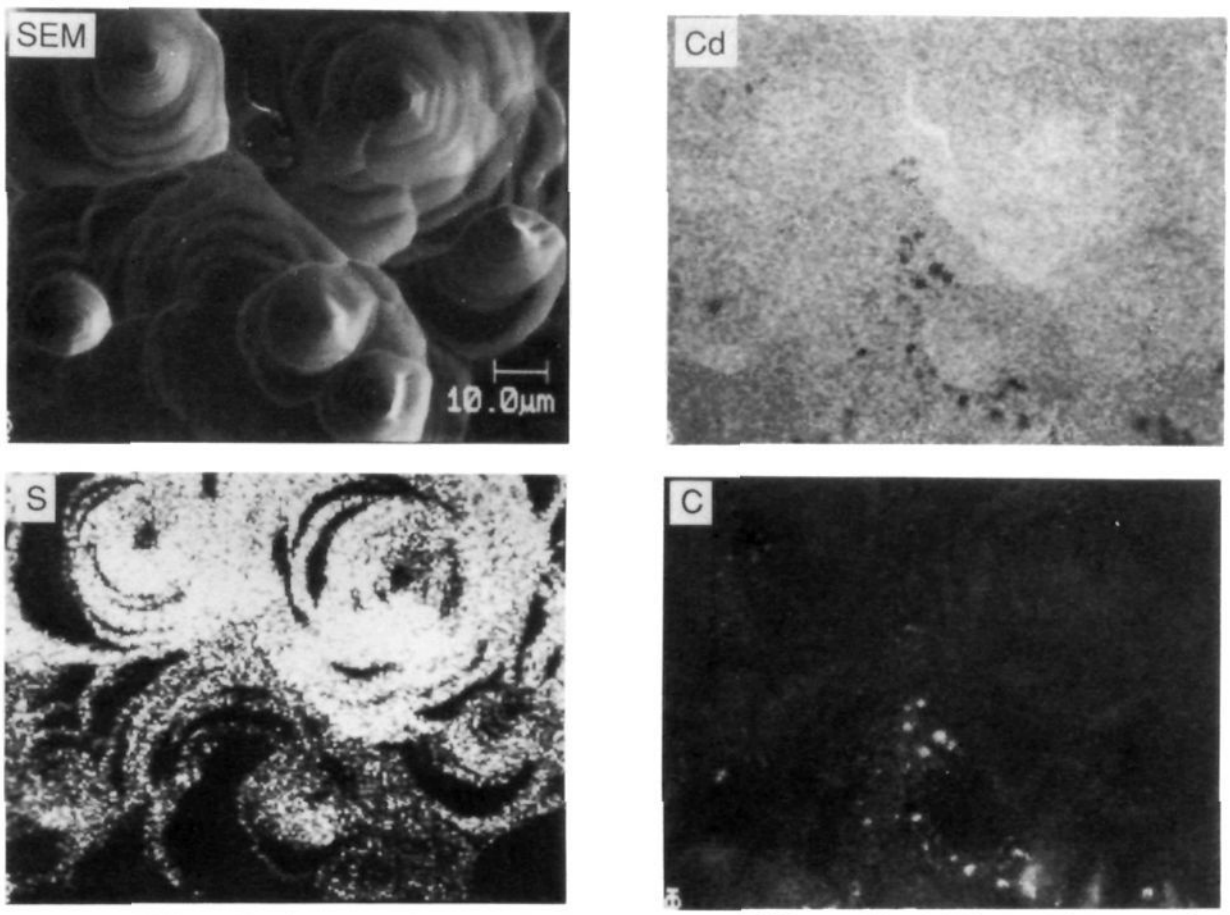

Figure 7. SEM and high lateral resolution Auger element maps (S, C, and Cd) of a second CdSe crystal ((0001) Cd face) modified with MoS_4^{2-}. The non-uniform S map shows non-uniform binding of the MoS_4^{2-}.

binding of $Et_2NCS_2^-$ on the Cd vs the S face would appear to be at least 3 to 1.

CdX/Electrolyte Interfaces. The correlation between surface orientation and binding of MoS_4^{2-} and $Et_2NCS_2^-$ indicates that there should also be crystal face dependent changes in the flat-band potential, E_{FB}, with the etched Cd-rich face showing a more negative shift than the etched S-rich face, cf. Scheme I. This is because E_{FB} of a semiconductor electrode is dependent on the amount of excess charge, Q_{ads}, due to adsorbed charged species on the surface. The excess charge at the semiconductor–solution interface causes a voltage drop across the Helmholtz layer, E_H, which is the same as the shift in E_{FB} of the semiconductor from its value in a non-interacting (innocent) electrolyte solution.[1,13,18] If it is assumed that the Helmholtz capacity, C_H, is constant (eq 2), it then follows that changes in the Helmholtz voltage induced by varying the solution concentration of the adsorbing species are

$$C_H = Q_{ads}/E_H \tag{2}$$

equal to changes in E_{FB}. Measured shifts in E_{FB} are then a direct measure of the extent of adsorption of charged species onto the semiconductor surface.

Measurement of interface capacitance versus potential provides a method to obtain values of E_{FB}.[18] The space charge capacitance, C_{sc}, of an ideal semiconductor/electrolyte interface should obey the Mott–Schottky relation (eq 3) at values of E_f where a depletion layer is formed. In eq 3, e is the electronic charge, ϵ is the semiconductor dielectric constant, ϵ_0 is the permittivity of free

$$\frac{1}{C_{sc}^2} = \frac{2}{e\epsilon\epsilon_0 N_D}\left(E_f - E_{FB} - \frac{kT}{e}\right) \tag{3}$$

space, and N_D is the donor density.[19] The literature values of ϵ are 10 for n-CdSe and 5.4 for n-CdS.[20] In the absence of deep donor levels or a high density of surface states, a plot of $1/C_{sc}^2$ vs E_f should be linear with the slope proportional to N_D and the x-axis intercept equal to E_{FB} (at room temperature, the correction for kT/e equals 27 mV). Reversible adsorption of a charged species will give parallel plots of $1/C_{sc}^2$ vs E_f with shifts related to the surface coverage. Nonparallel plots indicate changes in N_D which could signal irreversible chemical changes. We find good agreement with the Mott–Schottky relation for CdX/MoS_4^{2-} or $CdX/Et_2NCS_2^-$ for a measurement frequency in the range 1–10 kHz.

Figure 10 shows the Mott–Schottky plots for the Cd-rich face of CdX for several concentrations of $[Et_4N]_2MoS_4$ in CH_3CN/0.1 M $NaClO_4$. The plots for a given semiconductor electrode are parallel and linear, consistent with eq 3. The data show a more negative E_{FB} with increasing solution concentration of MoS_4^{2-}. Similar data are shown in Figure 11 for CdSe. The most negative E_{FB} values shown are −1.18 and −1.43 V vs Ag/Ag^+ at n-CdS and n-CdSe, respectively. In the absence of MoS_4^{2-}, the values of E_{FB} vs Ag/Ag^+ are −0.80 V for n-CdS and −0.60 V for n-CdSe.[1] Interestingly, the shifts in E_{FB} from adsorption of the dianion MoS_4^{2-} (0.4–0.9 V) are smaller, not larger, than found upon adsorption of the monoanion $Et_2NCS_2^-$ (~1.0 V).[1]

The electrodes prepared with the X-rich face exposed also give Mott–Schottky plots that are linear and parallel. However, a wide range of E_{FB} shifts was recorded upon addition of 5×10^{-2} M MoS_4^{2-}. In some cases, the magnitude of the shift was 50% of that seen for cases where the Cd-rich face was exposed. However, it is found that the shift of E_{FB} for the S-rich face depends on how long the surface is etched, whereas the shift of E_{FB} for Cd-rich

(18) Morrison, S. R. *Electrochemistry at Semiconductor and Oxidized Metal Electrodes*; Plenum: New York, 1980; p 49.

(19) Myamlin, V. A.; Pleskou, Y. V. *Electrochemistry of Semiconductors*; Plenum: New York, 1967.

(20) Sze, S. M. *Physics of Semiconductor Devices*; Wiley: New York, 1981.

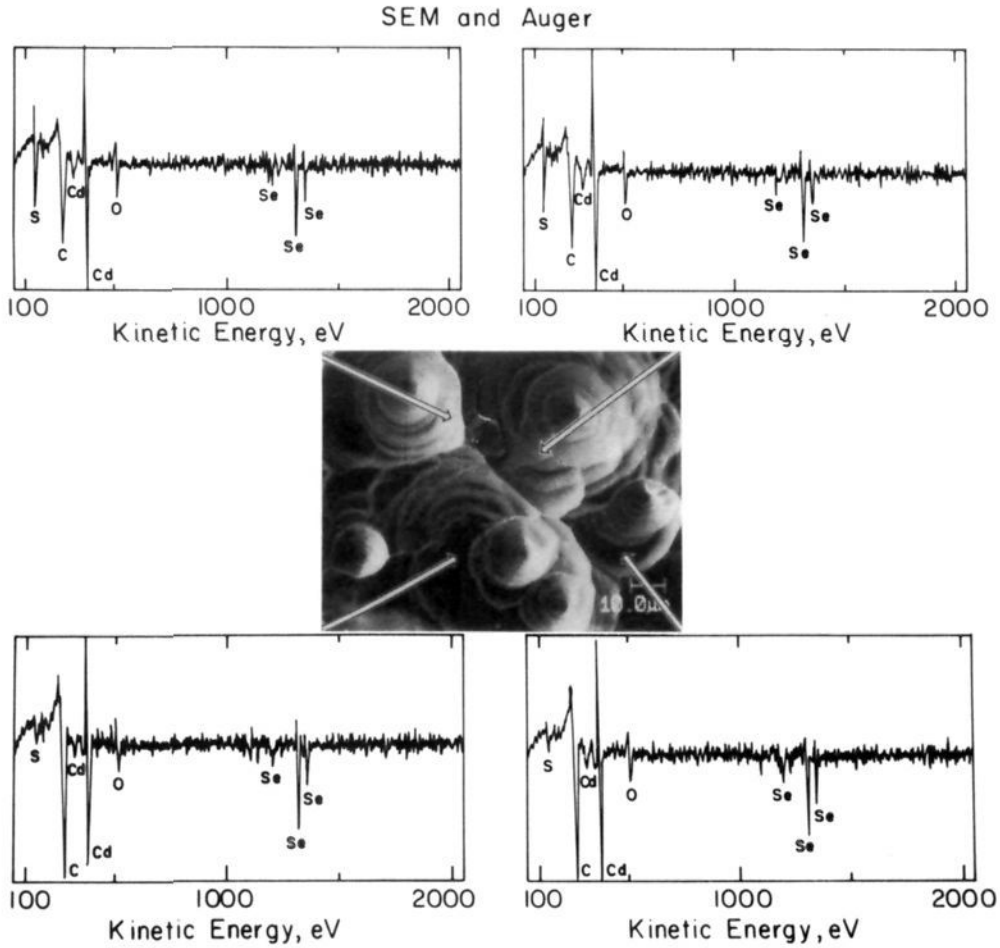

Figure 8. SEM of the Cd-rich face of the CdSe single crystal shown in Figure 7. Survey Auger scans were performed in a region of the S map indicating high coverage (top scans) and where low S coverage is found in the S element maps of Figure 7 (bottom scans). The S/Cd ratio in the top scans is consistent with about a monolayer of MoS_4^{2-}.

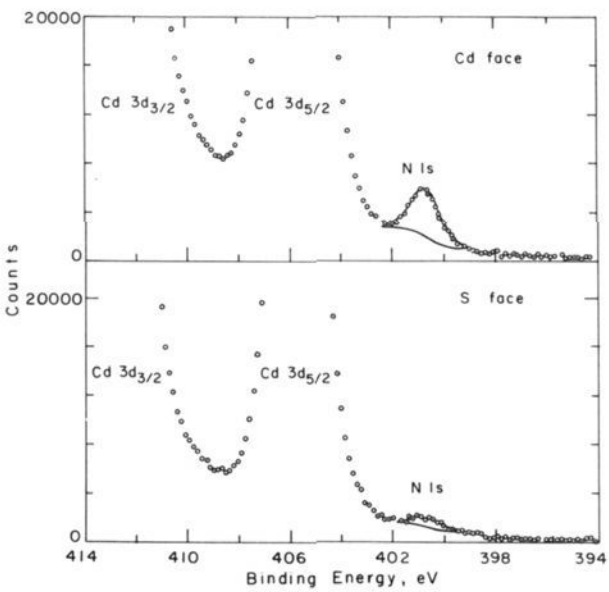

Figure 9. Comparison of XPS data for the Cd and S faces of (0001) CdS after treatment with $Et_2NCS_2^-$ showing adsorption preferentially on the Cd-rich face, based on the relative intensity of the N 1s signal.

faces is essentially independent of the degree of etching after the first etch. Figure 12 shows the effect of prolonged etching of the S-rich face on the shift of E_{FB} found from interaction with MoS_4^{2-}. In particular, a 30-s etch of the S-rich face yields little change in E_{FB}, whereas a 30-s etch for a Cd-rich surface shows a very

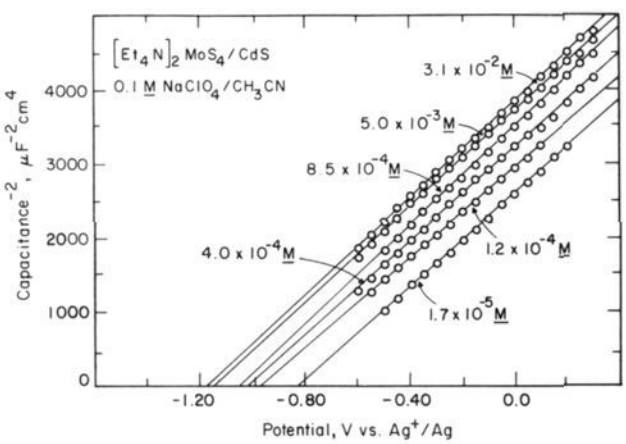

Figure 10. Plots of $1/C^2$ vs electrode potential at different concentrations of $[Et_4N]_2MoS_4$ at the Cd-rich face of CdS.

large negative shift of E_{FB}. Thus, the large shift of E_{FB} on the Cd-rich face does correlate with the selective binding of MoS_4^{2-} deduced from surface analysis. Our AES maps (Figures 5–8) show that binding of MoS_4^{2-} is non-uniform even on the Cd-rich face, and thus it is not surprising that prolonged etching of the S-rich face ultimately reveals binding sites. Others have attributed differences in efficiency of CdX-based photoelectrochemical cells to differing chemical etch procedures.[4e,21,22] The etching yields

(21) (a) Ellis, A. B.; Kaiser, S. W.; Wrighton, M. S. *J. Am. Chem. Soc.* **1976**, *98*, 1635. (b) Heller, A.; Chang, K. C.; Miller, B. *J. Electrochem. Soc.* **1977**, *124*, 697.

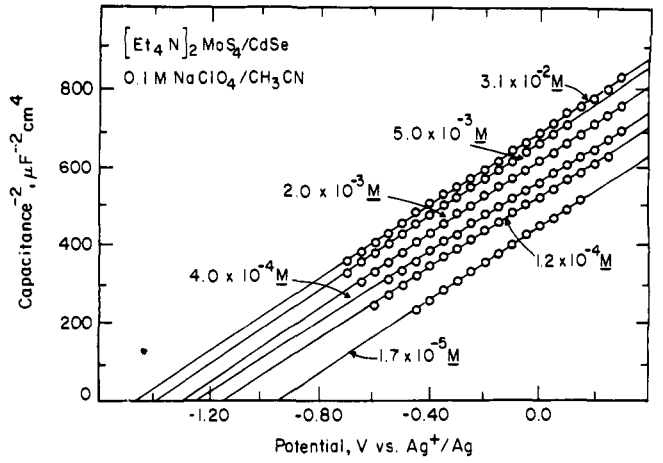

Figure 11. Plots of $1/C^2$ vs electrode potential at different concentrations of $[Et_4N]_2MoS_4$ at the Cd-rich face of CdSe.

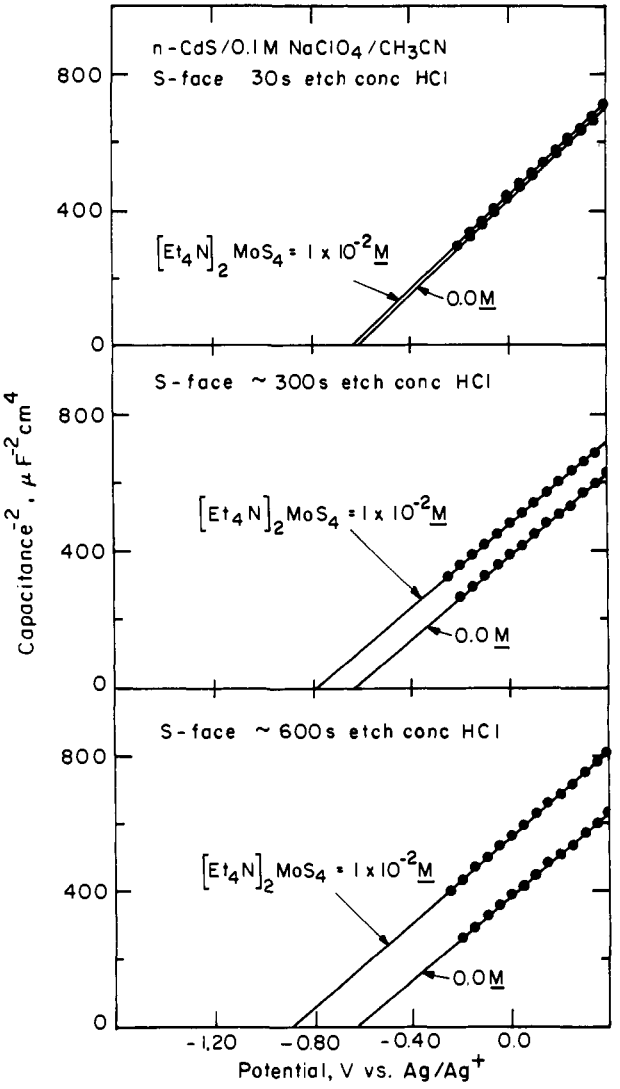

Figure 12. Plots of $1/C^2$ vs electrode potential for the S-rich face of a single CdS crystal in electrolyte at $[MoS_4^{2-}] = 0$ and in electrolyte at $[MoS_4^{2-}] = 1 \times 10^{-2}$ M after etching for 30, 300, or 600 s in 12 M HCl.

much larger negative shifts in E_{FB} on either the Cd- or X-rich face resulting in larger photovoltages. These researchers have not been able to correlate the increase in photovoltage with increases in surface area and have concluded that other factors may

(22) (a) Tenne, R.; Hodes, G. *Appl. Phys. Lett.* **1980**, *37*, 428. (b) Hodes, G. *Nature* **1980**, *285*, 29. (c) Tenne, R. *Appl. Phys.* **1981**, *25*, 13. (d) Liu, G. J.; Olsen, J.; Saunders, D. R.; Wang, J. H. *J. Electrochem. Soc.* **1981**, *128*, 1224.

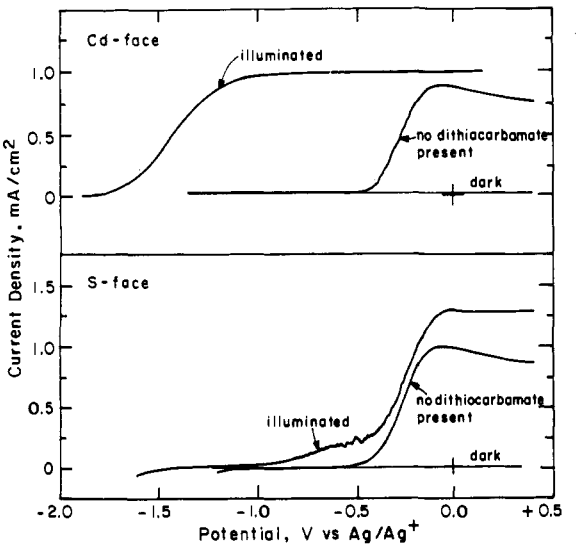

Figure 13. Steady-state photocurrent–voltage curves for 0.05 M Na-$[Et_2NCS_2]$ in 0.1 M $NaClO_4/CH_3CN$ at the Cd face of CdS (top) and the S face of CdS (bottom) while illuminating with the 488-nm line of an Ar laser.

be involved such as removal of recombination centers at the surface.[23] However, the improved (more negative) E_{FB} upon etching may be due to exposure of a greater number of binding sites for the anionic redox reagent.

Photocurrent–voltage curves can also be used to gauge the effect of anionic S donors on E_{FB}. The onset of photocurrent can be taken as a rough guide to E_{FB}.[1,13,18] The photoelectrochemical oxidation of MoS_4^{2-} at Cd-rich surfaces does show a very negative onset of oxidation, consistent with the E_{FB} measured from the Mott–Schottky plots. However, the oxidation of MoS_4^{2-} results in the deposition of the product (unidentified) onto the electrode. The photoelectrochemical oxidation of $Et_2NCS_2^-$ was also examined at both faces of freshly etched (30 s) (0001) CdS. This is a good system to examine, because large, reproducible shifts in E_{FB} at the Cd-rich face have been previously reported,[1] and the photooxidation product is soluble. In addition, the $Et_2NCS_2^-$ is optically transparent at the wavelengths where CdS absorbs, whereas MoS_4^{2-} is not. The CdS electrodes used for the photocurrent–voltage measurements in the presence of $Et_2NCS_2^-$ experiments were contacted on an edge such that either face could be exposed to solution. The face not being examined was covered with paraffin wax. Figure 13 shows the photocurrent–voltage curves for the Cd-rich face (top) and S-rich face (bottom) of the same CdS electrode. The Cd-rich face gives results similar to previous work:[1] the $Et_2NCS_2^-$ has a strong effect on the photocurrent onset, consistent with a very negative E_{FB} due to adsorption of $Et_2NCS_2^-$. In contrast, the S-rich face is little affected by the added $Et_2NCS_2^-$. However, upon further etching of the S-rich face, we find a negative shift of E_{FB} and improved rectangularity of the photocurrent–voltage curve, but not to the extent seen with the Cd-rich face. Thus, the superior performance of the Cd-rich face correlates with selective interaction of $Et_2NCS_2^-$ established by XPS (Figure 9). Repeated etching of the S-rich face does yield substantial improvements in E_{FB}, in accord with the etching dependence of the interface capacitance (Figure 12).

Conclusions

Surface analysis, capacitance, and photocurrent–voltage curves for n-type (0001) CdX (X = S, Se) show that anionic S donors interact selectively with the Cd-rich face. High lateral resolution AES shows that the binding of MoS_4^{2-} is non-uniform on the Cd-rich face of CdSe. Examination of the etch pits shows remarkable degrees of selectivity of binding to certain faces. The apparent selectivity for binding for MoS_4^{2-} or $Et_2NCS_2^-$ depends on the extent to which the crystal is etched. The etched X-rich

(23) Hodes, G. In *Energy Resources through Photochemistry and Catalysis*; Gratzel, M., Ed.; Academic Press: New York, 1983; p 421.

surfaces eventually present binding sites for the anionic S donors, but the precise nature of such sites is not clear. Future studies are to be directed toward studies of other crystal orientations to establish the scope and origins of selective binding, but it is clear that freshly etched (0001) CdX shows strong adsorption of MoS_4^{2-} and $Et_2NCS_2^-$ on the Cd-rich face which yields a very large effect on E_{FB}.

Considering the high degree of non-uniform binding of MoS_4^{2-} on the etched Cd-rich face of CdSe, we intend to investigate the distribution of adsorbates or reactants in other instances, including CdS,[24] GaAs,[25-27] and InP,[28] where surface modification yields physical and chemical changes or significant improvements in photoelectrochemical cells. Our data show that the AES technique is useful in detecting ~1 monolayer converages at a lateral resolution of <1 μm on the semiconductor surfaces. We have previously demonstrated AES to be useful for mapping surface composition of Au or Pt microelectrodes on Si_3N_4 substrates at <1-μm resolution for molecular monolayers.[29] For the modified semiconductor surfaces an aim is to relate non-uniform coverage of adsorbates with electrochemical behavior. For example, our observations are consistent with frequency-dependent interfacial capacitance measurements[30] which have been interpreted to mean that the Cd face of (0001) CdS is composed of regions with different values of E_{FB}.

A final point of interest concerns the magnitude of E_{FB} shifts for CdS and CdSe for MoS_4^{2-} vs $Et_2NCS_2^-$.[1] We find that the MoS_4^{2-} results in a larger shift on the Cd-rich face of CdSe (0.7–0.9 V) than on CdS (0.4–0.6 V) whereas it has been found[1] that $Et_2NCS_2^-$ yields a similar shift (~1 V) on CdS and CdSe. These differences, albeit modest in some ways, suggest that very subtle structural factors govern the coordination of the anionic S donors on CdX. The more highly charged MoS_4^{2-} does not lead to a larger shift in E_{FB} than found for $Et_2NCS_2^-$; in fact, the shift is somewhat smaller! A systematic study of $R_2NCS_2^-$ derivatives if planned, in order to establish steric and electronic effects on the binding of the dithiocarbamates to CdX.

Acknowledgment. We thank the United States Department of Energy, Office of Basic Energy Sciences, Division of Chemical Sciences for support of this research. We acknowledge use of XPS and Auger facilities acquired through the joint Harvard/M.I.T. University Research Initiative funded by the Defense Advanced Research Projects Agency.

Registry No. CdS, 1306-23-6; CdSe, 1306-24-7; MoS_4^{2-}, 16330-92-0; $Et_2NCS_2^-$, 147-84-2; HCl, 7647-01-0; $[Et_4N]_2MoS_4$, 14348-09-5; Na-$[Et_2NCS_2]$, 148-18-5.

(24) (a) Meyer, G. J.; Leung, L. K.; Yu, J. C.; Lisensky, G. C.; Ellis, A. B. *J. Am. Chem. Soc.* **1989**, *111*, 5146. (b) Campbell, B. D.; Farnsworth, H. E. *Surf. Sci.* **1968**, *10*, 197.

(25) Parkinson, B. A.; Heller, A.; Miller, B. *Appl. Phys. Lett.* **1978**, *33*, 521.

(26) Abrahams, I. L.; Tufts, B. J.; Lewis, N. S. *J. Am. Chem. Soc.* **1987**, *109*, 3472.

(27) Tufts, B. J.; Abrahams, I. L.; Santangelo, P. G.; Ryba, G. N.; Casagrande, L. G.; Lewis, N. S. *Nature* **1987**, *326*, 861.

(28) Spool, A. M.; Daube, K. A.; Mallouk, T. E.; Belmont, J. A.; Wrighton, M. S. *J. Am. Chem. Soc.* **1986**, *108*, 3155.

(29) (a) Hickman, J. J.; Zou, C.; Ofer, D.; Harvey, P. D.; Wrighton, M. S.; Laibinis, P. D.; Bain, C. D.; Whitesides, G. M. *J. Am. Chem. Soc.* **1989**, *111*, 7271. (b) Laibinis, P. D.; Hickman, J. J.; Wrighton, M. S.; Whitesides, G. M. *Science (Washington, DC)* **1989**, *245*, 845. (c) Hickman, J. J.; Ofer, D.; Zou, C.; Laibinis, P. E.; Whitesides, G. M.; Wrighton, M. S. *J. Am. Chem. Soc.* **1991**, *113*, 1128.

(30) Braun, C. M.; Fujishima, A.; Honda, K. *Chem. Lett.* **1985**, 1763.

Proton Affinity Ladders from Variable-Temperature Equilibrium Measurements. 1. A Reevaluation of the Upper Proton Affinity Range

Michael Meot-Ner (Mautner)* and L. Wayne Sieck*

Contribution from the Chemical Kinetics Division, National Institute of Standards and Technology, Gaithersburg, Maryland 20899. *Received October 10, 1990. Revised Manuscript Received January 23, 1991*

Abstract: An interlocking ladder of relative proton affinities of 47 compounds, over a range of 54 kcal/mol, was obtained from the enthalpies of proton-transfer equilibria, by using variable-temperature pulsed high-pressure mass spectrometry. From C_3H_6 (PA = 179.5 kcal/mol) to i-C_4H_8 (PA = 195.9 kcal/mol) the results agree well with tabulated values, but for the upper PA range the present values are increased significantly. For example, the present vs literature PA values are NH_3, 208.3 vs 204.0; CH_3NH_2, 219.6 vs 214.1; and t-$C_4H_9NH_2$, 229.2 vs 220.8 kcal/mol. The new value for t-$C_4H_9NH_2$ is also confirmed by the association thermochemistry of t-$C_4H_9^+$ with NH_3. The entropies of protonation are in reasonable agreement with expected rotational symmetry changes. Aromatics and olefins show a positive entropy of protonation of 3–6 cal/mol K due to structural effects, but no anomalous effects are observed that would indicate a dynamic proton.

Introduction

The gas-phase basicities, i.e., $-\Delta G°$ of protonation, of approximately 800 compounds have been measured, compiled, and evaluated.[1] Most of the data were derived from relative gas-phase basicities (i.e., $\Delta G°$ measurements), as given by the equilibrium constant of reaction 1.

$$AH^+ + B \rightleftharpoons BH^+ + A \quad (1)$$

In the great majority of measurements, equilibria 1 were determined at a single temperature, and the thermochemistry was derived from relations 2 and 3.

$$\Delta G° = -RT \ln K \quad (2)$$

$$\Delta G° = \Delta H° - T\Delta S° \quad (3)$$

In order to derive the thermochemistry from measured ln K values, the temperature at which the measurements were done must be assigned. Many of the early ICR measurements were carried out at ambient temperatures, originally assumed to be 300 K. Later, several authors revised their data to take the heating

(1) Lias, S. G.; Liebman, J. F.; Levin, R. D. *J. Phys. Chem. Ref. Data* **1984**, *13*, 695.